Evolving Processing Speed Asymmetries and Hemispheric Interactions in a Neural Network Model

Alexander Grushin, James A. Reggia

{agrushin,reggia}@cs.umd.edu

Department of Computer Science, University of Maryland, College Park, MD

20742, USA

Abstract

Substantial experimental data suggests that the cerebral hemispheres have different processing speeds, and that this may contribute to hemispheric specialization. Here, we use evolutionary computation models to examine whether asymmetric hemispheric processing speeds and lateralization can emerge in neural networks from the need to respond quickly to stimuli and/or to minimize energy consumption. Simulated neuroevolution produced networks with left-right asymmetric processing speeds whenever fitness depended on energy minimization, but not on quickness of response. The results also provide support for a recent hypothesis that subcortical cross-midline interactions are inhibitory/competitive.

1

1. Introduction

The underlying causes of cerebral hemispheric specializations, where one hemisphere performs a task better than the other, are not well understood at present [2]. While the many known underlying neurobiological asymmetries are presumed to be relevant, which actually contribute to hemispheric specialization, and the role of hemispheric interactions via the corpus callosum, remain unanswered questions. A substantial number of neural models of emergent cerebral specialization have been created over the last fifteen years, where deliberately-introduced asymmetries led to lateralization during learning [7]. However, these past studies have generally not examined how these asymmetries arose during evolution.

Here, we ask: Why might the presence of underlying hemispheric asymmetries be beneficial to the brain from an evolutionary point of view [9]? We evolve the parameters in a genetic representation of interacting left and right hemispheric regions to identify conditions under which underlying asymmetries

will emerge, and subsequently, during learning/development, lead to behavioral specialization. We extend [9] by using evolutionary multiobjective optimization methods [10] to examine the specific hypotheses: 1. hemispheric regions will evolve to have asymmetrical processing speeds [5] if they must both learn to perform well during a developmental period, and at the same time, minimize energy utilization and/or response time [1,3,8]; and 2. inhibitory cross-midline influences will also evolve under these conditions [6].

2. Methods

The neural networks used in this study (Figure 1) have a very simplified architecture motivated by top-level brain structure. Input patterns activate the left and right subcortical regions, which compute their activation in an iterative fashion, with both regions iterating simultaneously, although perhaps at separate frequencies. After one unit of time, the subcortical regions stop iterating, and pass their results to the cortical regions, which iterate for another time unit, and then activate the output region, which iterates either until each output neuron is on or off within a tolerance of 0.2, or for a maximum of three time units. The kth iteration of region X with a frequency of F_X iterations per time unit (where $1 \leq k \leq F_X$) is performed at time k/F_X, where $X \in \{LS, RS, LC, RC, OUT\}$ in Figure 1.

3

During a single iteration, each neuron i in a region computes a linearly-weighted sum h_i of its incoming synaptic activity. Activation levels a_i are then updated as follows: $a_i \leftarrow a_i + \delta[\sigma(h_i) - a_i]$, where $\sigma(x) = (1+e^{-x})^{-1}$, and $\delta = 0.1$. Iterative activation dynamics allow opposite regions to influence each other across interhemispheric connections. Feedforward weights are initially random in [-1, 1], and subsequently trained via standard error backpropagation. Weight modifications are based on errors in the output region (measured after all iteration terminates), which are backpropagated through the hidden regions as they would be in a more standard, non-iterative feedforward network. Training is done for 300 epochs in a per-pattern fashion, with a learning rate of 0.2.

The uniform weights W_{CM}, W_{CC} of interhemispheric connections and the iteration frequencies F_X of the hidden regions ($F_{OUT} = 20$ for all networks) do not change during training, but are instead determined over a larger time scale by a genetic algorithm (tournament size 3 for selection; 50 generations; population size 50; crossover, mutation, and reproduction-only probabilities 0.5, 0.4, and 0.1, respectively). The evolved parameters (Table 1; S is the random number generator seed, which determines the initial weights, and is included in the chromosome for a fully deterministic fitness evaluation process) are encoded as a sequence of real numbers in the range [0, 1], and realized via a linear mapping. Because of the enormous computational cost of repeatedly training populations of

4

networks, we used very small regions: $|IN| = 8$; $|LS| = |RS| = 10$; $|LC| = |RC| = 15$; and $|OUT| = 6$.

For every generation of the evolutionary process, the fitness of each chromosome is evaluated by instantiating a network with phenotypic parameter values that are based on its genome, and training it, using supervised learning, on a set of 16 pairs (taken from [9]) of input vectors in $\{0, 1\}^8$ and target output vectors in $\{0, 1\}^6$. The network's post-training performance on this same set is then gauged using the metrics of root-mean-square error (E); response time (t_r), which is the number of time units necessary for the output neurons to satisfy the termination conditions, averaged over all patterns; and energy consumption, which has two alternative definitions, one (J_{act}) depending on activation levels within the subcortical/cortical regions, and the other (J_{freq}) based on the iteration frequencies of those regions:

$$J_{act} = 1/P \cdot \Sigma_{p \in P}[(\Sigma_{X \in \{LS,RS,LC,RC\}}[|X|^2 \Sigma_{i \in X} o_{pi}^2]) / (\Sigma_{X \in \{LS,RS,LC,RC\}}[|X|^3])]$$

$$J_{freq} = (\Sigma_{X \in \{LS,RS,LC,RC\}}[|X| \cdot F_X])^2 / (\Sigma_{X \in \{LS,RS,LC,RC\}}[|X| \cdot F_X^{max}])^2$$

Here, P is the set of input patterns; o_{pi} is the final observed activation value for neuron i, given pattern p; and F_X^{max} is the maximum possible iteration frequency of region X (20 in all cases). Based on the above cost metrics, four objectives

(fitness criteria) to be maximized were: accuracy $\equiv 2 - E$; speed $\equiv 4 - t_r$ (note the distinction between "speed" – a behavioral measure, and "frequencies", a.k.a. "processing speeds", which are evolved); activity-based energy efficiency $\equiv 2 - J_{act}$; and frequency-based energy efficiency $\equiv 2 - J_{freq}$. In the experiments reported here, six different fitness functions were used: I. accuracy alone; II. accuracy and speed; III. accuracy and activity-based energy efficiency; IV. accuracy and frequency-based energy efficiency; V. accuracy, speed, and activity-based energy efficiency; and VI. accuracy, speed, and frequency-based energy efficiency. For the multiobjective fitness functions II – VI, fitness during evolution is determined by the *Strength Pareto Evolutionary Algorithm* (SPEA) [10], an evolutionary multiobjective optimization technique. SPEA maintains a set of "best" networks (of size ten in our experiments), with an emphasis on a diverse sampling of various objective tradeoffs.

Ten independent runs of the genetic algorithm were performed with each fitness function I – VI. Each run had an initial population that was generated with a distinct stream of random numbers. For each of the ten best networks returned under I and the 100 networks produced for II – VI, the error E_L (E_R) was measured with only the left (right) hemisphere contributing to the output. Early termination was not used during this process; rather, each time a network was activated on pattern p, its output region was made to iterate the exact same

number of times that it iterated when both sides were contributing. The

lateralization coefficient ρ [4] used in this study was computed as $\rho = |\,[E_L–E_R]\,/$

$[2 – (E_L+E_R)/2]\,|$, and ranged from values very close to 0.0 (virtually no

lateralization), to over 0.8 for the most lateralized networks. The asymmetry

coefficient α was also calculated as follows: $\alpha = s_\rho \cdot |\,[F_{LS}+F_{LC}–F_{RS}–F_{RC}]\,/$

$[F_{LS}+F_{LC}+F_{RS}+F_{RC}]\,|$, where $s_\rho = 1$ if $[E_R–E_L]$ and $[F_{LS}+F_{LC}–F_{RS}–F_{RC}]$ do not have

opposite signs, and $–1$ otherwise. Informally, a negative value of α indicates that

the lower-frequency regions are more accurate. Values for α exceed 0.9 in cases

of very strong asymmetry, and are 0.0 for perfectly symmetric networks.

3. Results

Table 2 gives the mean (μ) and standard deviation (σ) measures computed

over all networks (one per run for I and ten per run for II – VI) produced by each

of ten runs for every fitness function. Pre-training error values were generally

well above 1.0, with no early termination ($t_r = 3$). Consistent with [9], the use of

accuracy alone in fitness function I did not produce strong asymmetries or

lateralization, although mild asymmetries were present, suggesting that perfect

synchronization in the iteration of opposite regions is not necessarily optimal for

good accuracy. Each hemisphere performed very poorly by itself, indicating that

the network's good post-training performance relies on interhemispheric

cooperation. Fitness function II, based on both accuracy and speed (quickness of

response) also did not result in strong asymmetries and lateralization; in fact, the

networks tended to be even more symmetric. Iteration frequencies were typically

high in all regions (about 19 on average), reflecting the fact that both accuracy

and speed of response can benefit from high processing speeds. Therefore, E and

t_r did not represent major tradeoffs, but were largely complementary.

In contrast to the above, strong asymmetries and lateralization arose whenever

either energy measure was incorporated into the fitness function (III – VI). The

model could achieve a reasonable level of accuracy while saving on energy (the

two being strongly-conflicting objectives) by reducing the computational

resources of one hemisphere and relying heavily on the other (more so than by

moderately reducing resource consumption in both hemispheres). As shown in

Figure 2, the values of asymmetry α and lateralization ρ measures are especially

high for networks where a "compromise" between accuracy and energy efficiency

occurs. For example, fitness based on accuracy and activity-based energy

efficiency (III) yielded highest values of α and ρ in the energy use range of [0.10

– 0.15], which corresponds to error values that are low, but not minimal among

the evolved networks. In this range, *extreme* asymmetries can occur in individual

networks, where the subcortical/cortical regions have an update frequency of 20

on one side, and 1 on the other. Asymmetry and lateralization values become progressively smaller as this compromise is shifted in favor of energy efficiency, because the dominant hemisphere tends to become slower as well. The results for the fitness functions based on three objectives (V, VI) are not drastically different from the corresponding results produced under III and IV. Once again, greatest asymmetry and lateralization values are observed for networks in the moderate energy consumption range, which balances with moderate-to-high accuracy and moderate-to-low speed levels, the latter criteria being positively correlated, and therefore, complementary.

Finally, in all cases, there was a tendency for inhibitory subcortical cross-midline connections to evolve ($W_{CM} < 0$). In contrast, callosal connections were excitatory ($W_{CC} > 0$) whenever energy use was not a factor in fitness (I, II), but were usually inhibitory when energy minimization was a factor (III – V). Interestingly, fitness function VI was the only one that produced strong lateralization with underlying asymmetries, inhibitory subcortical cross-midline connections, and an excitatory corpus callosum, a set of results argued to be most consistent with empirical data [6].

4. Discussion

9

While our results require confirmation and further study with larger and more realistic models, they are intriguing, and suggest a number of conclusions. First, when paired left and right neural pathways evolved with fitness based on just accuracy, or both accuracy and quickness of response, significant left-right asymmetry in hemispheric processing speeds and subsequent functional lateralization did not arise. This result does not provide support for the hypothesis that rapid responses to stimuli are an important factor in the emergence of brain asymmetries related to hemispheric processing speeds (e.g., [8]), but can be explained by the complementary relationship that exists between speed of response and accuracy within our model. Second, and in contrast, whenever minimization of energy consumption was a factor in determining fitness, considerable asymmetry in left versus right processing speeds appeared, and led to strong functional lateralization. This result is consistent both with substantial experimental data about asymmetrical hemispheric processing speeds [5] and with arguments that the minimization of energy use is an important factor in brain evolution [1,3]. Thus, our results suggest that tradeoffs between objectives, and not just objectives themselves, produce asymmetries and lateralization. Finally, in line with the earlier results of [9], while simulated callosal connections varied across fitness functions, simulated subcortical cross-midline connections typically evolved to be inhibitory under all conditions. These results are consistent with a

recent hypothesis that subcortical cross-midline inhibitory connections or other subcortical left-right competitive mechanisms may be much more important in causing hemispheric specialization than is generally recognized [6].

Acknowledgements

References

[1] A. Gibbons, Solving the Brain's Energy Crisis, Science 280 (1998) 1345-1346.

[2] J. Hellige, Hemispheric Asymmetry (Harvard University Press, 1993).

[3] S. Laughlin and T. Sejnowski, Communication in Neuronal Nets., Science 301 (2003) 1870-1874.

[4] M. Lezak, Neurological Assessment (Oxford University Press, 1995).

[5] M. Nicholls, Temporal Processing Asymmetries Between the Cerebral Hemispheres, Laterality 1 (1996) 97-137.

[6] J. Reggia et al., The Callosal Dilemma, Neurological Research 23 (2001) 465-

471.

[7] J. Reggia and S. Levitan, Hemispheric Interactions and Specialization, in: M. Arbib, ed., Handbook of Brain Theory and Neural Nets. (MIT Press, 2003) 525-528.

[8] L. Rogers, Evolution of Hemispheric Specialization, Brain and Language 73 (2000) 236-253.

[9] Y. Shkuro and J. Reggia, Cost Minimization During Simulated Evolution of Paired Neural Nets., Cog. Sys. Res. 4 (2003) 365-383.

[10] E. Zitzler and L. Thiele, Multiobjective Evolutionary Algorithms, IEEE Transactions on Evolutionary Computation 3 (1999) 257-271.

Alexander Grushin is a PhD student in Computer Science at the University of Maryland. His research interests include artificial neural networks, evolutionary algorithms, and particle swarms.

James A. Reggia received his PhD and MD degrees from the University of Maryland, where he is currently a Professor of Computer Science doing research in biologically-inspired computing and AI.

Figure 1: Network architecture. The regions are: input (IN), left/right subcortical (LS/RS), left/right cortical (LC/RC), and output (OUT). Dark arrows denote full feedforward connections, while light arrows denote subcortical cross-midline (CM) and corpus callosum (CC) connections, which are strictly pairwise. There are no intra-region connections.

Figure 2: Scatterplots for fitness functions III (top) and IV (bottom), showing asymmetry α ($\square$) and lateralization ρ ($\blacklozenge$) versus error (left), and energy use (right).

Table 1: Chromosome Description

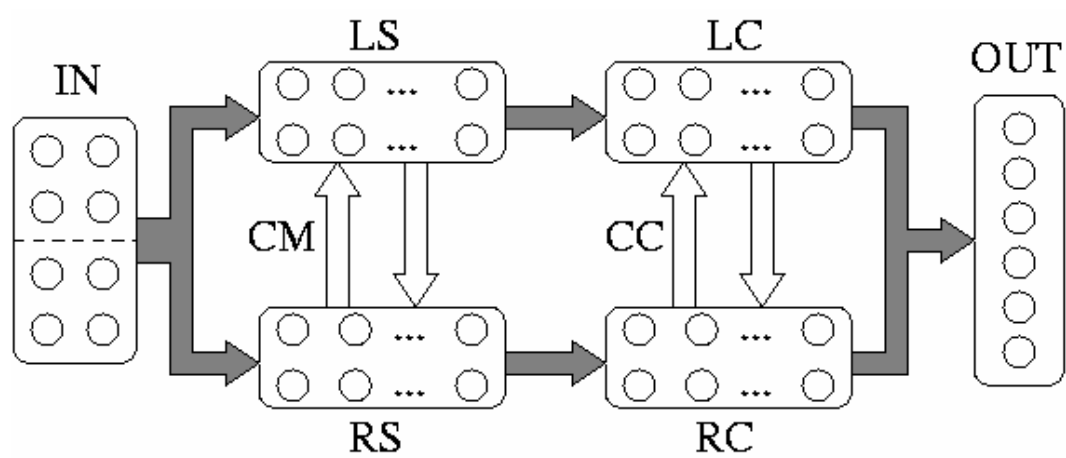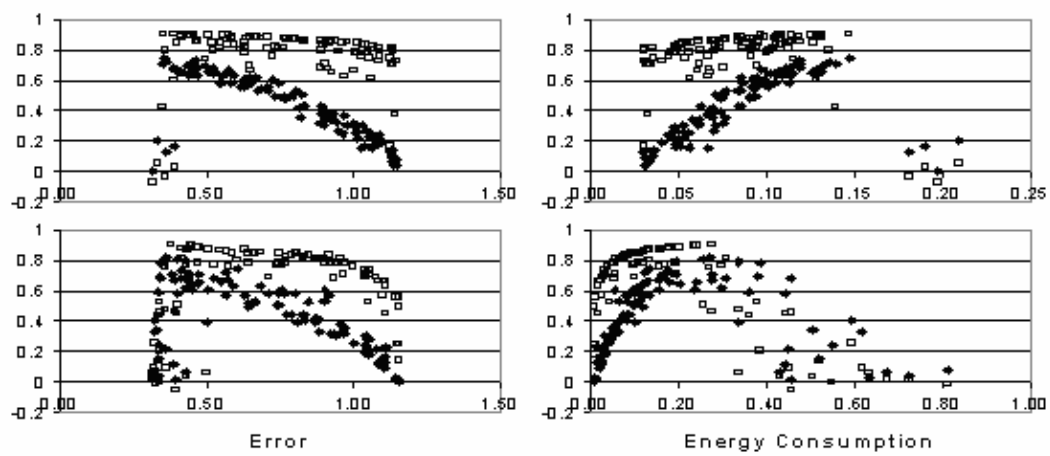**Table 2:** Experimental Measurements for Fitness Functions I – VI

Figure 1

Figure 2

Position	1	2	3	4	5	6	7
Parameter	S	F_{LS}	W_{CM}	F_{RS}	F_{LC}	W_{CC}	F_{RC}
Min. Value	0	1	-3.0	1	1	-3.0	1
Max. Value	10000000	20	3.0	20	20	3.0	20

Table 1

Measure	I		II		III		IV		V		VI	
	μ	σ	μ	σ	μ	σ	μ	σ	μ	σ	μ	σ
E	0.30	0.00	0.31	0.01	0.76	0.26	0.71	0.29	0.55	0.23	0.51	0.23
t_r	1.56	0.17	1.25	0.23	2.86	0.25	2.75	0.41	2.41	0.59	2.36	0.59
J_{act}	0.25	0.03	0.25	0.03	0.09	0.04	0.12	0.06	0.14	0.05	0.17	0.06
J_{freq}	0.83	0.10	0.91	0.07	0.21	0.14	0.18	0.19	0.43	0.29	0.35	0.22
W_{CM}	-1.65	1.48	-2.36	0.74	-1.34	1.94	-1.18	1.83	-1.54	1.65	-2.38	0.83
W_{CC}	0.98	1.81	0.99	2.13	-2.10	1.25	-0.35	2.19	-2.24	1.10	0.82	2.01
ρ	0.13	0.12	0.11	0.06	0.43	0.21	0.42	0.24	0.42	0.26	0.44	0.25
α	0.03	0.06	0.01	0.04	0.77	0.19	0.62	0.29	0.53	0.36	0.43	0.33

Table 2